Landslides (2021) 18:1875–1887
DOI 10.1007/s10346-020-01593-2
Received: 9 June 2020
Accepted: 20 November 2020
Published online: 7 January 2021

Fangwei Yu · Lijun Su

Experimental investigation of mobility and deposition characteristics of dry granular flow

Abstract This paper presents an experimental investigation of mobility and deposition characteristics of dry granular flow, by a number of flume tests on silica sand no. 3 and silica sand no. 7, to interpret the effects of angle of slope, granular volume, cushion, granular structure, and granular size on the mobility and deposition characteristics of granular flow. Along a given slope, an increase of the amount of sand impaired its mobility. However, for a given amount of sand along a slope, an increase of the angle of slope resulted in a V-shaped change of the angle of mass center movement, implying the existence of a characteristic combination of the angle of slope and the amount of sand to yield the maximum mobility of granular flow. The angle of mass center movement increased while increasing the thickness of cushion, showing that the cushion impaired the mobility of granular flow. Granular structure using the mixed structures of silica sand no. 3 and silica sand no. 7 affected greatly the mobility of granular flow, by showing an inverted structure in the near runout area with the deposition of the materials in the upper half of original grading structure in the far runout area for the inverse grading structure and normal grading structure. The mobility of granular flow increased with the change in turn of the inverse grading structure, the uniform structure, and the normal grading structure. The increase of the grain sizes of granular material enhanced its mobility. In addition, the angle of mass center movement showed a more reliable assessment for the mobility of granular flow in comparison with the angle of maximum mass movement.

Keywords Deposition · Flume tests · Granular flow · Mobility · Sands

Introduction

Granular flow is a theme of global focus as a common phenomenon in nature, e.g., landsides, debris flow, snow avalanche, rock avalanche, sand movement, and pyroclastic flow, showing a significant representation of natural hazards to life and property. In the process of granular flow, the gravity-induced energy of granular material is transformed into the kinetic energy by accelerating its movement along a slope before decelerating on a gentler slope where the interaction of granular particles dissipating energy overcomes the driving energy. In fact, it is always existence of the complex combination of the friction and collision among granular particles and slope in granular flow so as to yield the complex mechanical mechanism and movement process of granular material with the compression and shearing (e.g., Langroudi et al. 2010; Federico and Cesali 2019; Zuo et al. 2019; Buettner et al. 2020). As a result, a great number of studies have been conducted to understand the fundamental dynamics and mechanism of granular flow by using physical model tests (e.g., Farin et al. 2014; Choi et al. 2017; Gray 2018; Ng et al. 2018), numerical tests (e.g., Crosta et al. 2009; Zhou and Ng 2010; Zhou and Sun 2013; Jiang et al. 2018; Gray 2018), fundamental theories (e.g., Eisbacher 1979; Davies 1982; Cruden and Hungr 1986; Thornton 1997; Legros 2002; Campbell 2006; Gray 2018), and case studies (e.g., Hewitt 1988; Strom 2004; Boultbee et al. 2006).

The mobility and mechanism of granular flow are affected greatly by the angles of slope and its following slopes, the shape of channel, the grading and volume of granular material, the physico-mechanical properties of granular material, and its substrate including the cushion and entrainment with or without fluidizing medium (e.g., water, air, volcanic gas, fine particles), initial granular structure (e.g., inverse grading structure, normal grading structure, uniform structure), and gravitational settings that result from the complex geological settings and earth surface process, causing the extremely complex dynamics and mobility of granular flow (e.g., Cruden and Hungr 1986; Davies 1982; Davies and McSaveney 1999; Legros 2002; Crosta et al. 2009; Zhou and Ng 2010; Zhou and Sun 2013; Farin et al. 2014; Jiang et al. 2018; Gray 2018; Ng et al. 2018, 2019).

The runout distance and coverage of the final disposition depend greatly on the volume of granular rather than its drop height (Hsu 1975). An increase in granular volume resulted in an increase of the maximum runout distance of granular flow, but the maximum drop height just caused the scatter of the correlation of granular volume and its maximum runout distance (Davies 1982). In the submarine settings, the velocity of granular flow was partly controlled by the turbulent drag exerted by seawater on its surface, causing a rapid loss of the initial high velocity (Norem et al. 1990). However, in the subaerial settings, the granular flow with sufficient water content may transform into a debris flow (Iverson et al. 1997). The angle of maximum mass movement showed a decrease despite in a large scatter while increasing the granular volume (Legros 2002). In reality, it is of great interest using the angle of mass center movement to assess the mobility of granular flow, rather than using the angle of maximum mass movement that is also used frequently because of its much easier availability. In fact, the fundamental understanding of the mobility and deposition of granular flow still remains a great challenge, which should be investigated by a great number of further studies because of the realistic difficulties and complexity of the direct investigation of granular flow in nature (e.g., Berger et al. 2011; Schürch et al. 2011; McCoy et al. 2013). As a consequence, a question arises as to how dry granular flow behaves in small-scale physical model tests, which would be worthy of clarifying the mobility and deposition characteristics of dry granular flow by a comprehensively systematic investigation as a significant and valuable complement for the past studies.

The purpose of this study is to comprehensively investigate the mobility and deposition characteristics of dry granular (sand) flow, by a number of small-scale flume tests on silica sand no. 3 and silica sand no. 7, to interpret the effects of angle of slope, granular volume, cushion, granular structure, and granular size on the mobility and deposition characteristics of granular flow.

Materials and methods

In this paper, silica sand no. 3 and silica sand no. 7, as poorly-graded sands (ASTM D2487-11 2011), were employed in a number of flume tests for investigating their mobility and deposition characteristics. Figure 1 gives the grain size distributions of silica sand no. 3 and silica sand no. 7, showing a similarity of the grading shape by an approximate translation. The physical properties of silica sand no. 3 and silica sand no. 7 are listed in Table 1.

As shown in Fig. 2, the experimental flume was made by using a 10-mm-thick transparent acrylic resin board with its internal width of 0.12 m, height of 0.3 m, and length of 0.64 m. In Fig. 2, the flume was fixed stably on a level ground covered by a large graph paper, forming a slope of the designated angles, i.e., 15°, 30°, and 45°, followed by a level ground. A granular container, as displayed in Fig. 2, was formed in the top of the upper slope of the flume in the dimension of length 0.12 m, width 0.12 m, and height 0.3 m, by setting a gate that would be used for cease and release of granular (sand) materials. Flume tests were conducted by upwardly removing the gate of the granular container promptly to release the granular material, yielding a granular flow along a slope of the flume and the level ground with a final deposition.

In this paper, the flume tests were performed using granular materials, i.e., silica sand no. 3 and silica sand no. 7, in the designated weights of sands, i.e., 1500 g, 3000 g, and 4500 g, along the designed slopes of flume, i.e., 15°, 30°, and 45°, with the given thickness of cushion using silica sand no. 7 on the level ground, i.e., 0.000 m, 0.002 m, and 0.009 m, for comprehensively investigating the effects of angle of slope, granular volume, cushion, granular structure, and granular size on the mobility and deposition characteristics of granular flow. Table 2 shows a summary of the granular flow tests on silica sand no. 3 and silica sand no. 7. In this paper, the half-sized contour map of the deposition on the ground was adopted in view of its axial symmetry along a central axis of the horizontal runout direction, by showing the thickness of deposition on the runout ground of Cartesian coordinate system by the horizontal coordinate axis (horizontal distance D_h) and the vertical coordinate axis (vertical distance D_v) with an origin 0 as defined in Fig. 2(b). In addition, it is always existence of the scale effect in all physical model tests; i.e., the scale of the physical model tests plays inevitably its role in affecting the behavior of granular materials, including the flume tests of granular flow in this paper, implying the limitation that the results of this work may be existence of difference from the real granular flow. It should be expected that the physical model scale effect on the mobility and deposition of dry granular flow would be investigated by the further work.

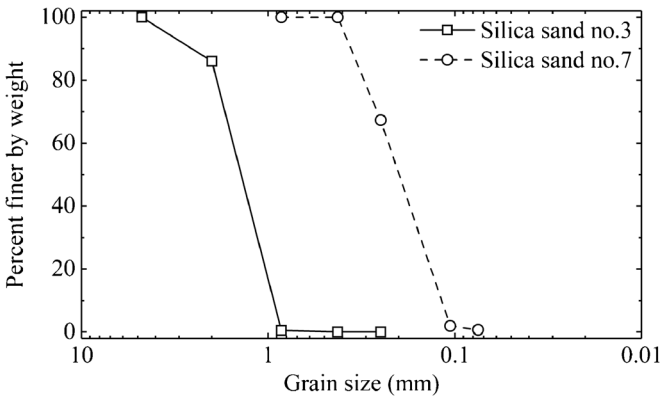

Fig. 1 Grain size distributions of silica sand no. 3 and silica sand no. 7

Table 1 Physical properties of silica sand no. 3 and silica sand no. 7

Property	Silica sands	
	No. 3	No. 7
Specific gravity, G_s[a]	2.619	2.641
Minimum void ratio, e_{min}[b]	0.699	0.700
Maximum void ratio, e_{max}[b]	0.987	1.211
Fines content, F_c[c]: %	0.000	0.680
Coefficient of uniformity, C_u[c]	1.687	1.888
Coefficient of curvature, C_c[c]	0.963	0.973
Classification[d]	SP	SP

[a] JGS 0111 (2015)

[b] JGS 0161 (2015)

[c] JGS 0131 (2015)

[d] ASTM D2487-11 (2011)

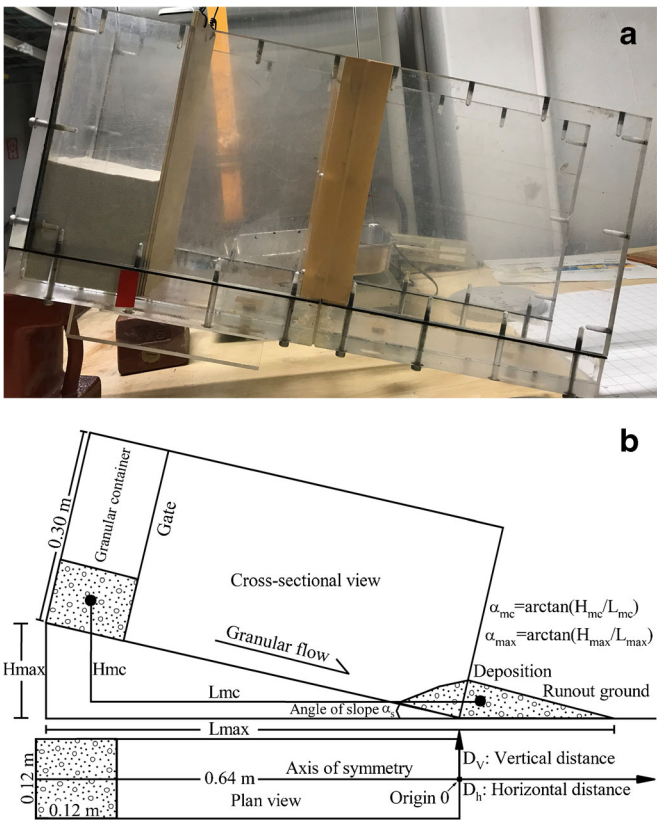

Fig. 2 Illustration of dry granular flow in flume test. **a** Photo of the used flume. **b** Dimension of the flume test with the definitions of the drop height of mass center H_{mc}, the runout distance of mass center L_{mc}, the maximum drop height of mass H_{max}, the maximum runout distance of mass L_{max}, the angle of mass center movement α_{mc}, the angle of maximum mass movement α_{max}, the horizontal distance D_h, the vertical distance D_v, and the origin 0

Table 2 Summary of the granular flow tests on silica sand no. 3 and silica sand no. 7

Materials	Angle of slope, α_s	Weight of sand, W	Dimension of sand, D	Thickness of cushion, T
Sand no. 7	15°	1500 g 3000 g 4500 g	0.12 m × 0.12 m × 0.09 m 0.12 m × 0.12 m × 0.18 m 0.12 m × 0.12 m × 0.27 m	0 m - no cushion
	30°	1500 g 3000 g 4500 g	0.12 m × 0.12 m × 0.09 m 0.12 m × 0.12 m × 0.18 m 0.12 m × 0.12 m × 0.27 m	0 m - no cushion
	45°	1500 g 3000 g 4500 g	0.12 m × 0.12 m × 0.09 m 0.12 m × 0.12 m × 0.18 m 0.12 m × 0.12 m × 0.27 m	0 m - no cushion
Sand no. 3	30°	1500 g 3000 g 4500 g	0.12 m × 0.12 m × 0.09 m 0.12 m × 0.12 m × 0.18 m 0.12 m × 0.12 m × 0.27 m	0 m - no cushion
	45°	1500 g 3000 g 4500 g	0.12 m × 0.12 m × 0.09 m 0.12 m × 0.12 m × 0.18 m 0.12 m × 0.12 m × 0.27 m	0 m - no cushion
	45°	1500 g 1500 g	0.12 m × 0.12 m × 0.09 m 0.12 m × 0.12 m × 0.09 m	0.02 m - sand no. 7 0.09 m - sand no. 7
Sand no. 7 Sand no. 3	45°	1500 g (case A) 1500 g (case B) 1500 g (case C)	0.12 m × 0.12 m × 0.18 m 0.12 m × 0.12 m × 0.18 m 0.12 m × 0.12 m × 0.18 m	0 m - no cushion

Case A: sand no. 3 750 g and sand no. 7 750 g mixed for uniformity

Case B: sand no. 3 750 g in the upper half and sand no. 7 750 g in the lower half

Case C: sand no. 3 750 g in the lower half and sand no. 7 750 g in the upper half

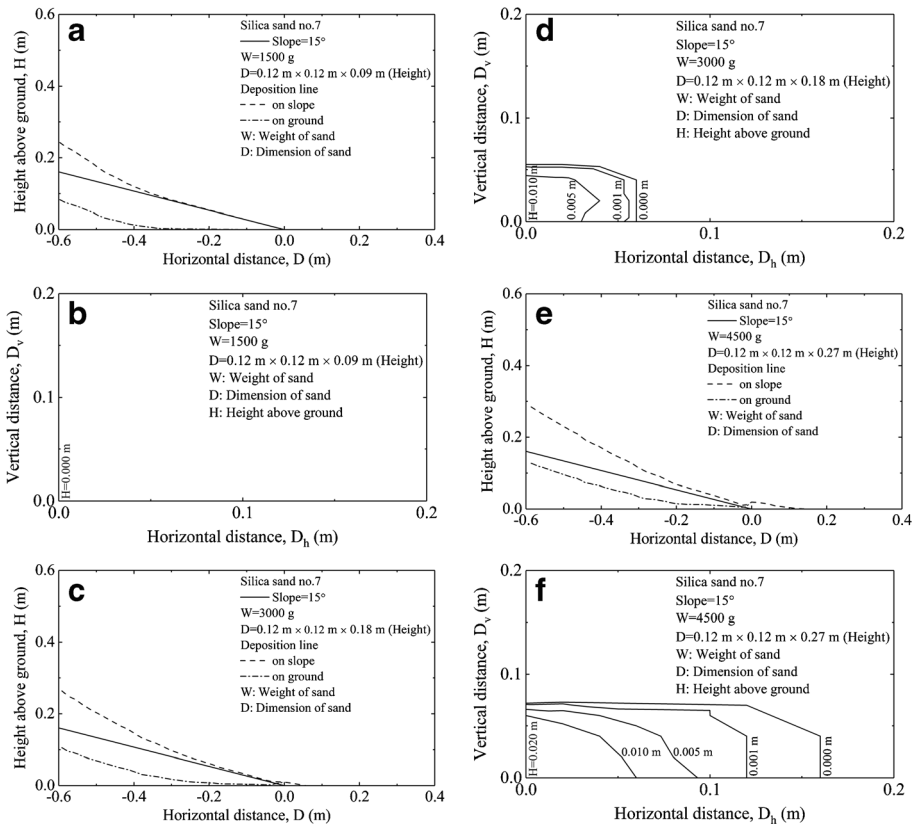

Fig. 3 Deposition of granular flow of silica sand no. 7 along a slope of 15°. **a** Deposition in height above ground against horizontal distance for sand 1500 g. **b** Deposition in vertical and horizontal distances for sand 1500 g. **c** Deposition in height above ground against horizontal distance for sand 3000 g. **d** Deposition in vertical and horizontal distances for sand 3000 g. **e** Deposition in height above ground against horizontal distance for sand 4500 g. **f** Deposition in vertical and horizontal distances for sand 4500 g

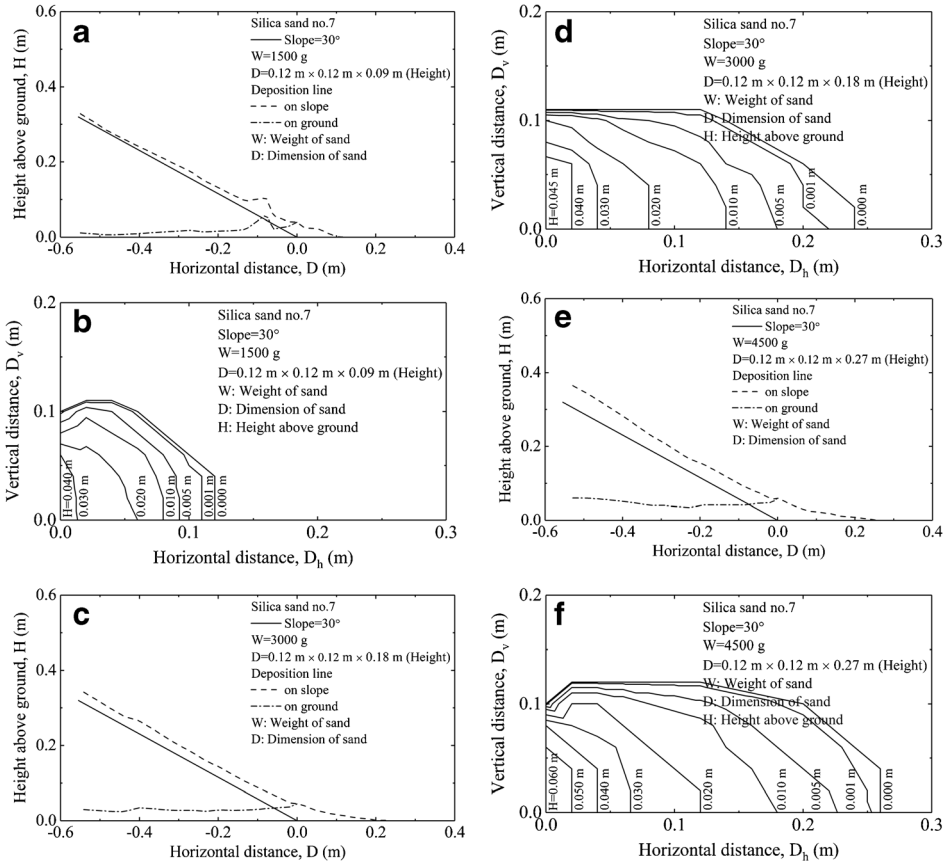

Fig. 4 Deposition of granular flow of silica sand no. 7 along a slope of 30°. **a** Deposition in height above ground against horizontal distance for sand 1500 g. **b** Deposition in vertical and horizontal distances for sand 1500 g. **c** Deposition in height above ground against horizontal distance for sand 3000 g. **d** Deposition in vertical and horizontal distances for sand 3000 g. **e** Deposition in height above ground against horizontal distance for sand 4500 g. **f** Deposition in vertical and horizontal distances for sand 4500 g

Results and discussion

Effect of angle of slope and granular volume on mobility and deposition of granular flow

Angle of slope and granular volume affect greatly the mobility and deposition of granular flow (e.g., Davies 1982; Legros 2002; Zhou and Ng 2010; Gray 2018; Ng et al. 2018). By picturing the deposition of granular flow of silica sand no. 7 1500 g, 3000 g, and 4500 g along a slope of 15°, in Fig. 3, it showed a larger and thicker deposition with a longer runout distance while increasing the amount of sand.

In Fig. 4, along a slope of 30°, silica sand no. 7 1500 g, 3000 g, and 4500 g were released for investigating the mobility and deposition characteristics, showing an approximately uniform deposition on the slope but a larger and thicker deposition on the level ground while increasing the amount of sand. In addition, the deposition on the level ground showed a gradual increase of the ratio of the horizontal runout distance—over—the vertical runout distance while increasing the amount of sand; i.e., the horizontal runout distance was influenced predominantly by the amount of sand in comparison with the vertical runout distance (e.g., Legros 2002; Farin et al. 2014).

Along a slope that was elevated to 45°, it showed, in Fig. 5, a different deposition line with a gradually increased coverage and thickness of the deposition while increasing the amount of sand. Angle of slope was revealed to play a great role in affecting the mobility and deposition characteristics of sand (e.g., Davies 1982; Legros 2002; Zhou and Sun 2013). For a given amount of silica sand no. 7, it showed, in Figs. 3, 4, and 5, an increase in the deposition coverage while increasing the angle of slope.

As a comparison with silica sand no. 7, silica sand no. 3 was also tested to investigate its mobility and deposition characteristics. In Fig. 6, it showed a gradual increase of the deposition coverage with increasing the amount of sand. However, the maximum thickness of the deposition showed an increase, i.e., from 0.045 to 0.060 m, followed by a constant at 0.060 m, while increasing the amount of sand. However, in Fig. 7, for silica sand no. 3 1500 g, 3000 g, and 4500 g along a slope of 45°, the deposition showed larger coverage with a gradually increased thickness with increasing the amount of sand.

By comparison of Fig. 6 and Fig. 7, along a given slope by a designated amount of silica sand no. 3, the coverage of the deposition on the ground increased monotonically with increasing the angle of slope. However, while increasing the angle of slope, the

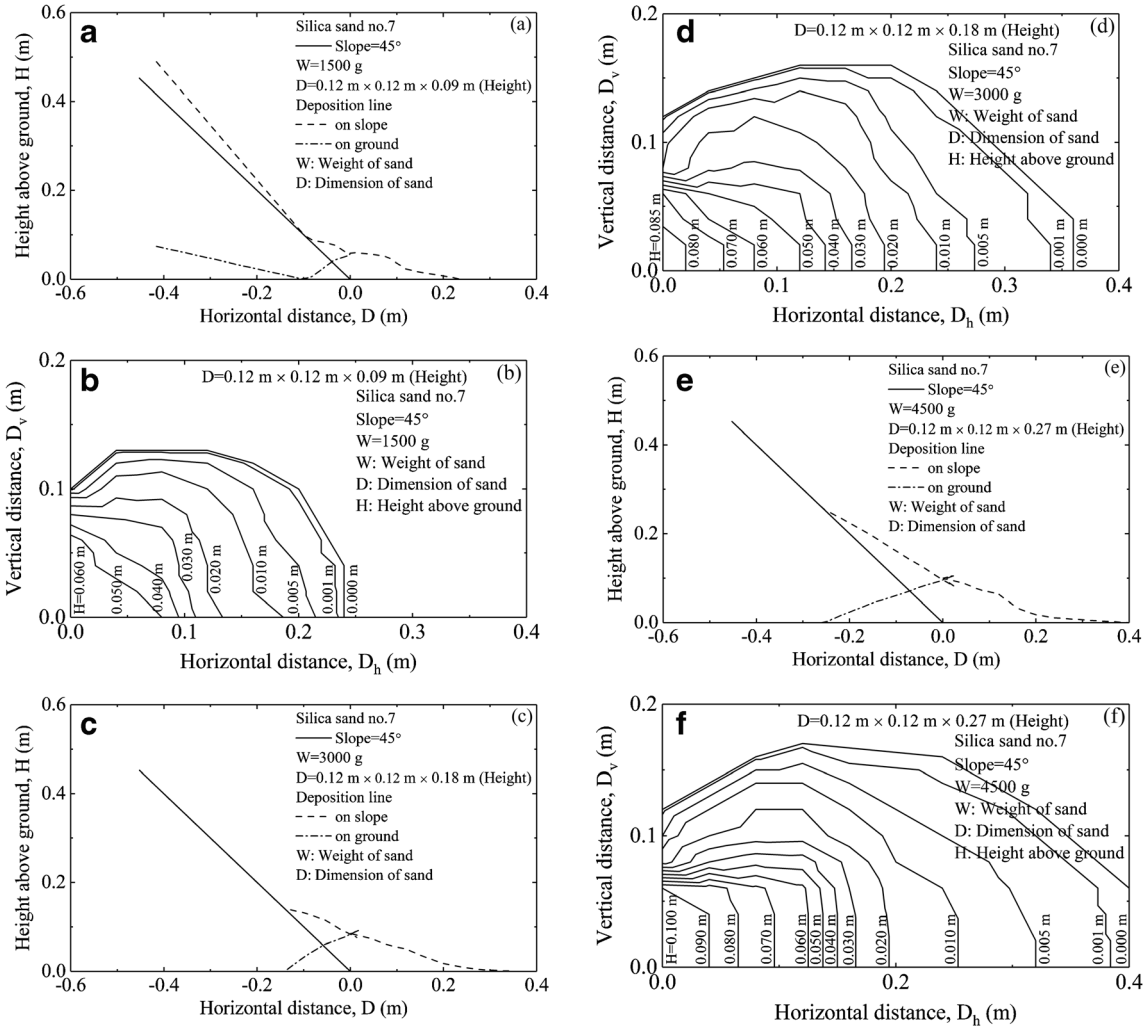

Fig. 5 Deposition of granular flow of silica sand no. 7 along a slope of 45°. **a** Deposition in height above ground against horizontal distance for sand 1500 g. **b** Deposition in vertical and horizontal distances for sand 1500 g. **c** Deposition in height above ground against horizontal distance for sand 3000 g. **d** Deposition in vertical and horizontal distances for sand 3000 g. **e** Deposition in height above ground against horizontal distance for sand 4500 g. **f** Deposition in vertical and horizontal distances for sand 4500 g

thickness of deposition on the ground showed an increase, expect for the tests of silica sand no. 3 1500 g that displayed a decrease of the thickness of the deposition on the ground.

Mobility of granular flow is always investigated by the drop height of mass center H_{mc}, the runout distance of mass center L_{mc}, the maximum drop height of mass H_{max}, and the maximum runout distance of mass L_{max} (e.g., Hsu 1975; Davies 1982; Legros 2002; Farin et al. 2014). In fact, the drop height of mass center H_{mc} and the runout distance of mass center L_{mc} are adopted most ideally to assess the mobility of granular flow in comparison with the maximum drop height of mass H_{max} and the maximum runout distance of mass L_{max} that are also usually used for assessing the mobility of granular flow because of the measurement difficulty of the drop height of mass center H_{mc} and the runout distance of mass center L_{mc} of granular flow in reality (e.g., Legros 2002; Berger et al. 2011; Schürch et al. 2011; McCoy et al. 2013).

Figure 8 shows the evolution of the drop height of mass against the runout distance of mass. In Fig. 8(a), the drop height of mass center showed a complex evolution against the runout distance of mass center for the tests of silica sand no. 7 and silica sand no. 3 subjected to the effects of angle of slope and amount of sand. However, in Fig. 8(b), while increasing the amount of sand, it showed a gradual increase of the maximum runout distance of mass at the constant maximum drop height of mass that increased with the increase of angle of slope, which follows the tendency of landslides that controlled its runout distance by its spreading, hence by its volume (Davies 1982). By comparison with silica sand no. 7, silica sand no. 3 showed a larger maximum runout distance of mass.

The ratio of the drop height of mass and the runout distance of mass is always employed to quantify the mobility of granular flow, with measuring the angle of mass movement that was defined by the angle of mass center movement α_{mc} (i.e., $\alpha_{mc} = \arctan(H_{mc}/L_{mc})$) or the angle of maximum mass movement α_{max} (i.e., $\alpha_{max} = \arctan(H_{max}/L_{max})$). Figure 9 shows the drop height—over—runout distance against the weight of sand. In Fig. 9(a), the ratio of the drop height of mass center and the runout distance of mass showed monotonic increase with increasing the amount of sand, despite of

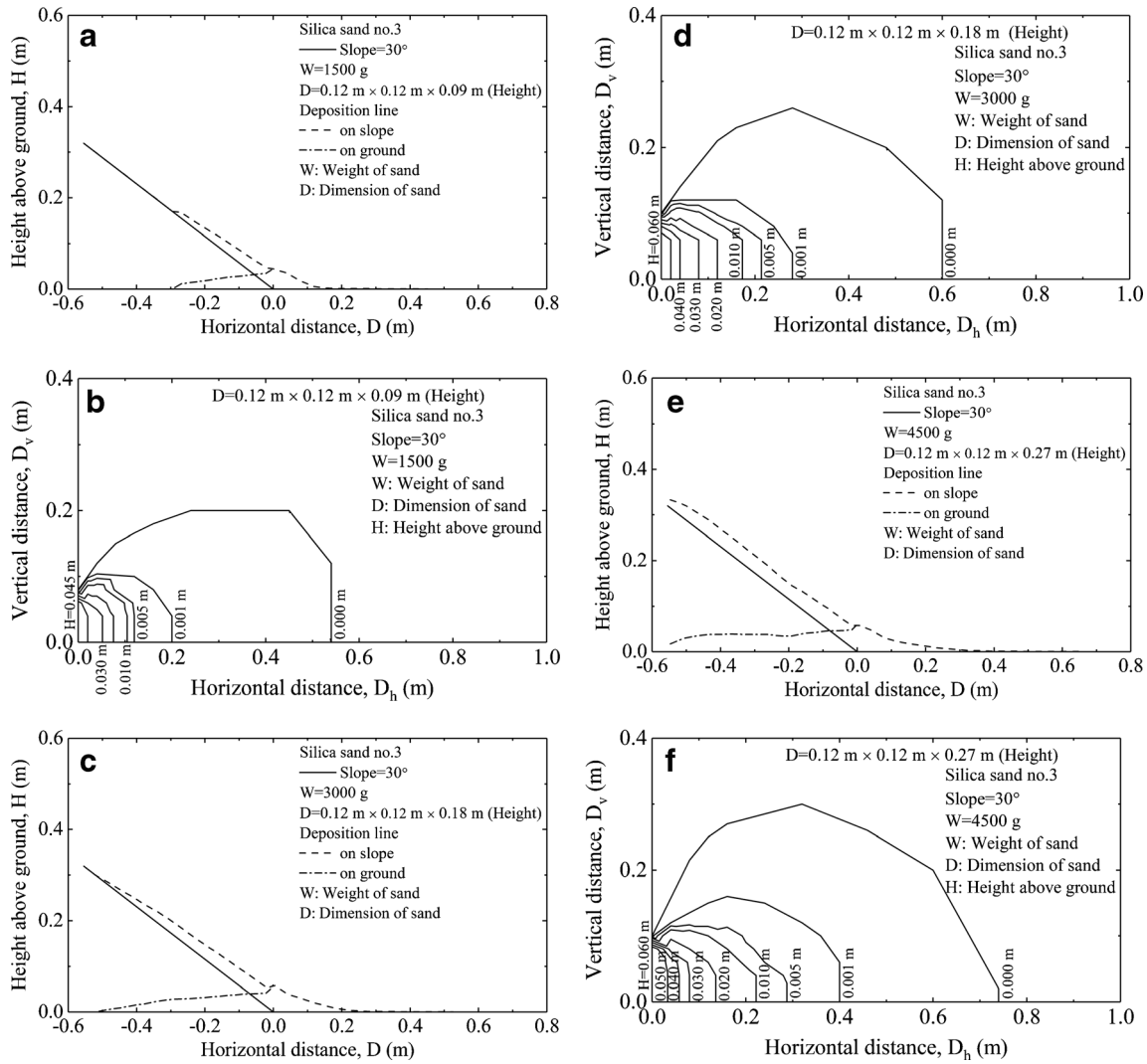

Fig. 6 Deposition of granular flow of silica sand no. 3 along a slope of 30°. **a** Deposition in height above ground against horizontal distance for sand 1500 g. **b** Deposition in vertical and horizontal distances for sand 1500 g. **c** Deposition in height above ground against horizontal distance for sand 3000 g. **d** Deposition in vertical and horizontal distances for sand 3000 g. **e** Deposition in height above ground against horizontal distance for sand 4500 g. **f** Deposition in vertical and horizontal distances for sand 4500 g

the types of sands and the angles of slopes. However, in Fig. 9(b), an increase of the amount of sand resulted in decrease of the ratio of the maximum drop height of mass and the maximum runout distance of mass, which showed a consistent tendency with a great number of landslides (Legros 2002).

In Fig. 10(a), along a given slope, the angles of mass movement α_{mc} showed an increase while increasing the amount of sand, implying that the increased amount of sand impaired its mobility, which is contrary to the evolution of the angles of mass movement α_{max} against the weight of sand in Fig. 10(b); i.e., the angles of mass movement α_{max} decreased as amount of sand increased, showing an increase of the mobility of sand. In addition, it shows larger angles of mass movement α_{mc} in comparison with the angles of mass movement α_{max}, revealing that the lower apparent friction coefficients for many landslides are from the lower angles of mass movement α_{max} (e.g., Davies 1982; Legros 2002). It should be noted that, the angle of mass movement α_{mc} is regarded as being more reliable assessment for the mobility of granular flow in comparison with the angle of mass movement α_{max}, indicating that the angle of mass movement α_{max} as a relatively lower angle of mass movement may not be acceptable for quantifying the mobility of granular flow in reality.

Effect of angle of slope on mobility and deposition of granular flow

Mobility of granular flow was investigated by the drop height—over—runout distance against angle of slope and its corresponding angle of mass movement against the angle of slope to investigate the effect of angle of slope, as shown in Figs. 11 and 12. For a given amount of sand, in Figs. 11(a) and 12(a), the drop height of mass center—over—the runout distance of mass center and its corresponding angle of mass movement α_{mc} showed a V-shaped evolution against the increase of angle of slope, i.e., in experiencing an initial decrease and then an increase while increasing the angle of slope, implying the

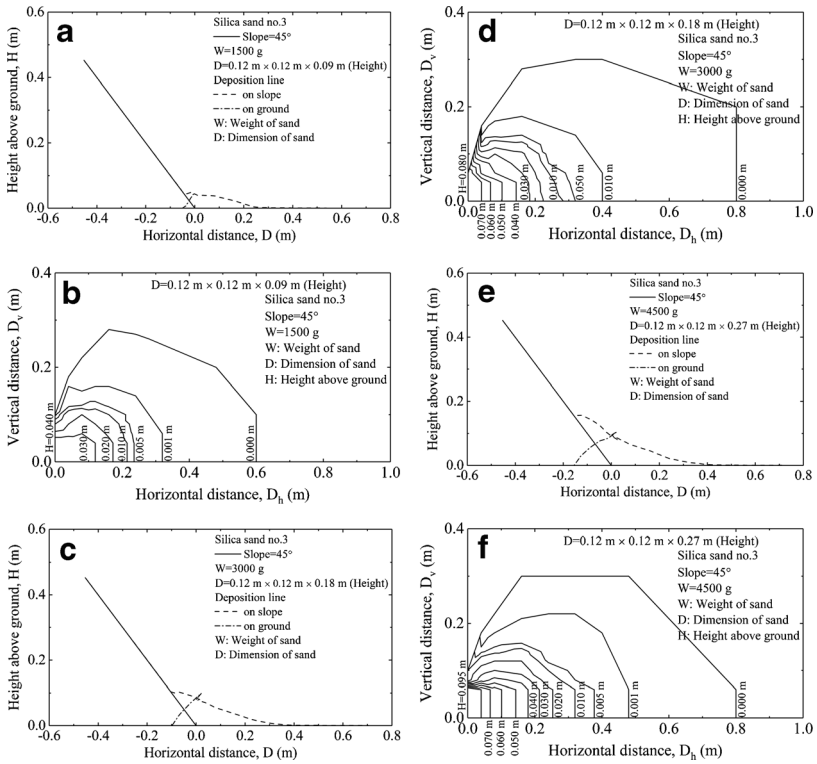

Fig. 7 Deposition of granular flow of silica sand no. 3 along a slope of 45°. **a** Deposition in height above ground against horizontal distance for sand 1500 g. **b** Deposition in vertical and horizontal distances for sand 1500 g. **c** Deposition in height above ground against horizontal distance for sand 3000 g. **d** Deposition in vertical and horizontal distances for sand 3000 g. **e** Deposition in height above ground against horizontal distance for sand 4500 g. **f** Deposition in vertical and horizontal distances for sand 4500 g

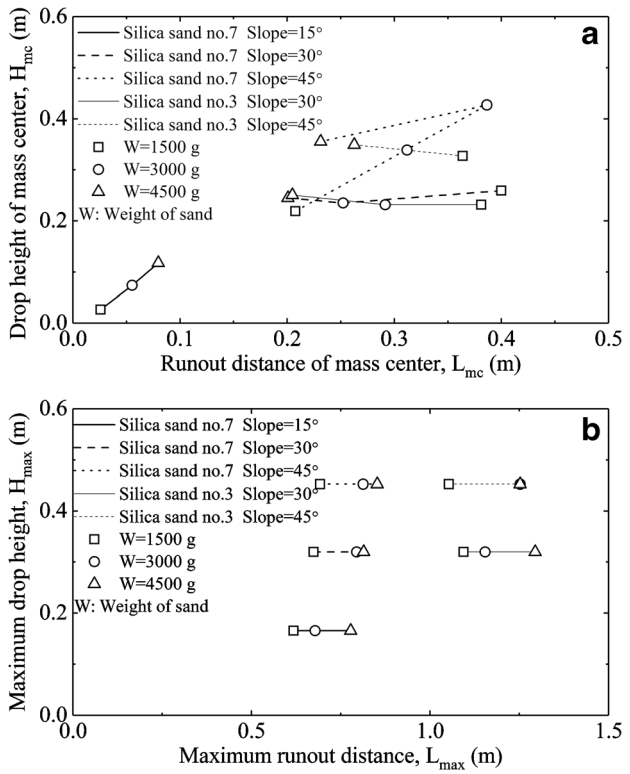

Fig. 8 Drop height of mass against runout distance of mass. **a** Drop height of mass center against runout distance of mass center. **b** Maximum drop height of mass against maximum runout distance of mass

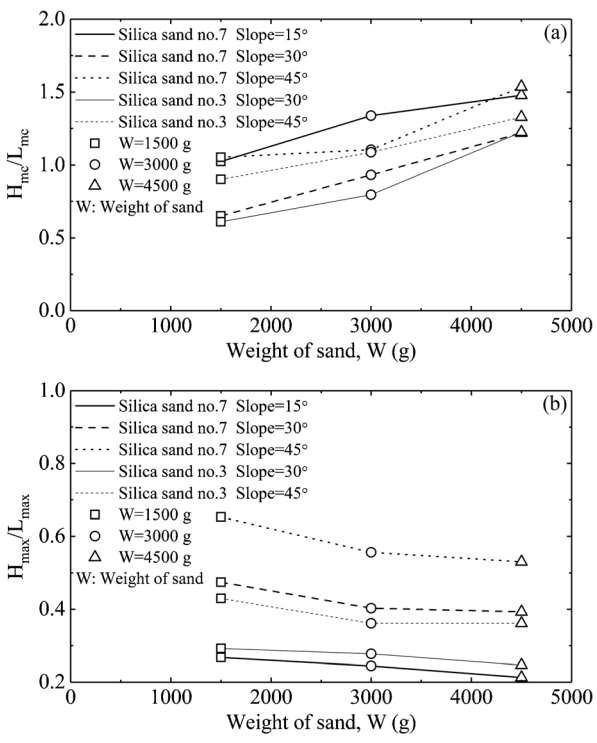

Fig. 9 Drop height—over—runout distance against weight of sand. **a** Drop height of mass center—over—runout distance of mass center against weight of sand. **b** Maximum drop height of mass—over—maximum runout distance of mass against weight of sand

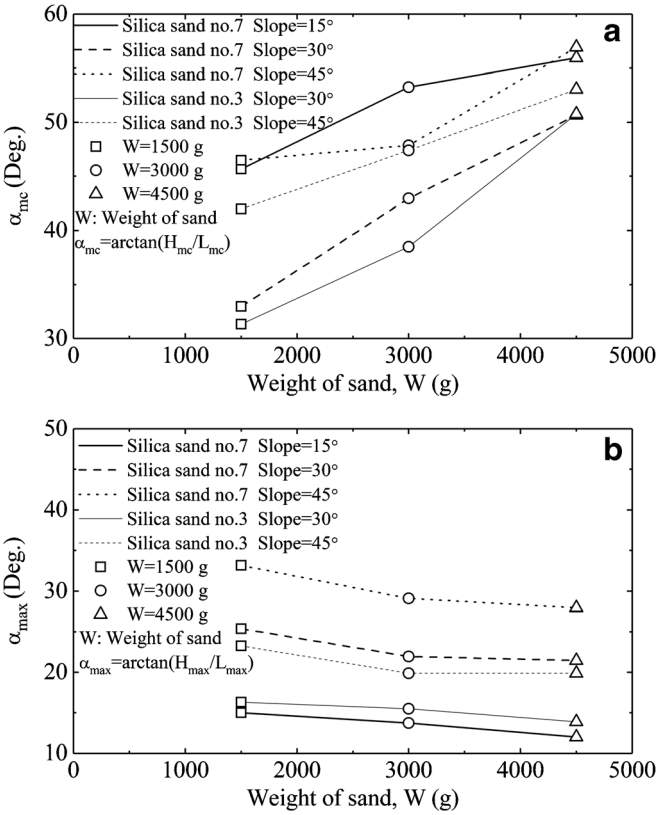

Fig. 10 Angle of mass movement against weight of sand. **a** Angle of mass center movement against weight of sand. **b** Angle of maximum mass movement against weight of sand

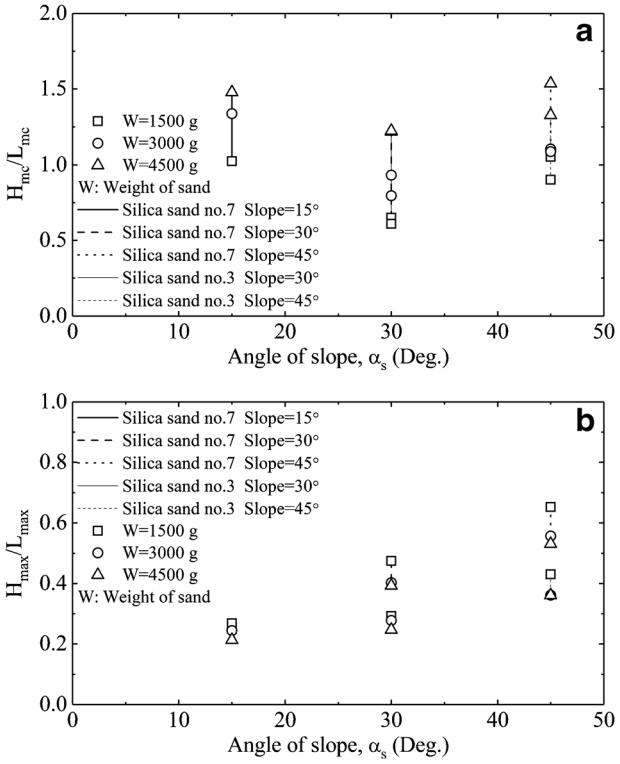

Fig. 11 Drop height—over—runout distance against angle of slope. **a** Drop height of mass center—over—runout distance of mass center against angle of slope. **b** Maximum drop height of mass—over—maximum runout distance of mass against angle of slope

existence of a characteristic combination of the angle of slope and the amount of sand to yield the maximum mobility of granular flow. However, in Figs. 11(b) and 12(b), the maximum drop height of mass—over—the maximum runout distance of mass and its corresponding angle of mass movement α_{max} showed a gradual increase with increasing the angle of slope, which is completely different from the evolution of the drop height of mass center—over—the runout distance of mass center and its corresponding angle of mass movement α_{mc} against the angle of slope in Figs. 11(a) and 12(a).

Effect of cushion on mobility and deposition of granular flow

In reality, granular soils may flow on a ground covered by granular material as a cushion that greatly affects the mobility of granular flow by changing its flow dynamics and deposition characteristics, with strong implications for granular flow hazard assessment (e.g., Legros 2002; Crosta et al. 2009; Farin et al. 2014). For clarifying the effect of cushion on mobility and deposition of granular flow, three flume tests were conducted by using silica sand no. 3 1500 g along a slope of 45° but with setting different thickness of silica sand no. 7 as a cushion on the level ground, i.e., 0.000 m, 0.002 m, and 0.009 m, as shown in Fig. 13. In Fig. 13, it showed a decrease of the coverage of deposition by shortening the runout distance to thicken the deposition while increasing the thickness of cushion, implying that the cushion impaired greatly the mobility of granular flow by dissipating the dynamic energy of granular flow.

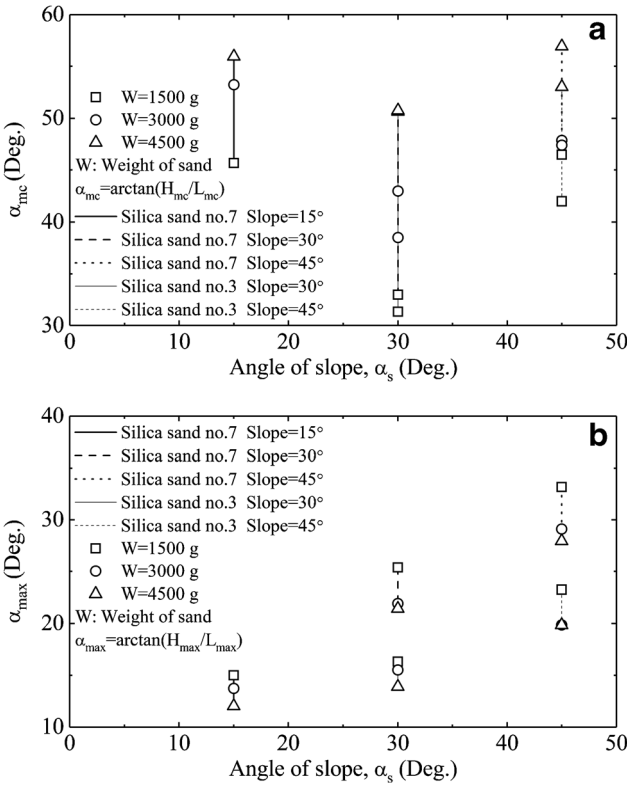

Fig. 12 Angle of mass movement against angle of slope. **a** Angle of mass center movement against angle of slope. **b** Angle of maximum mass movement against angle of slope

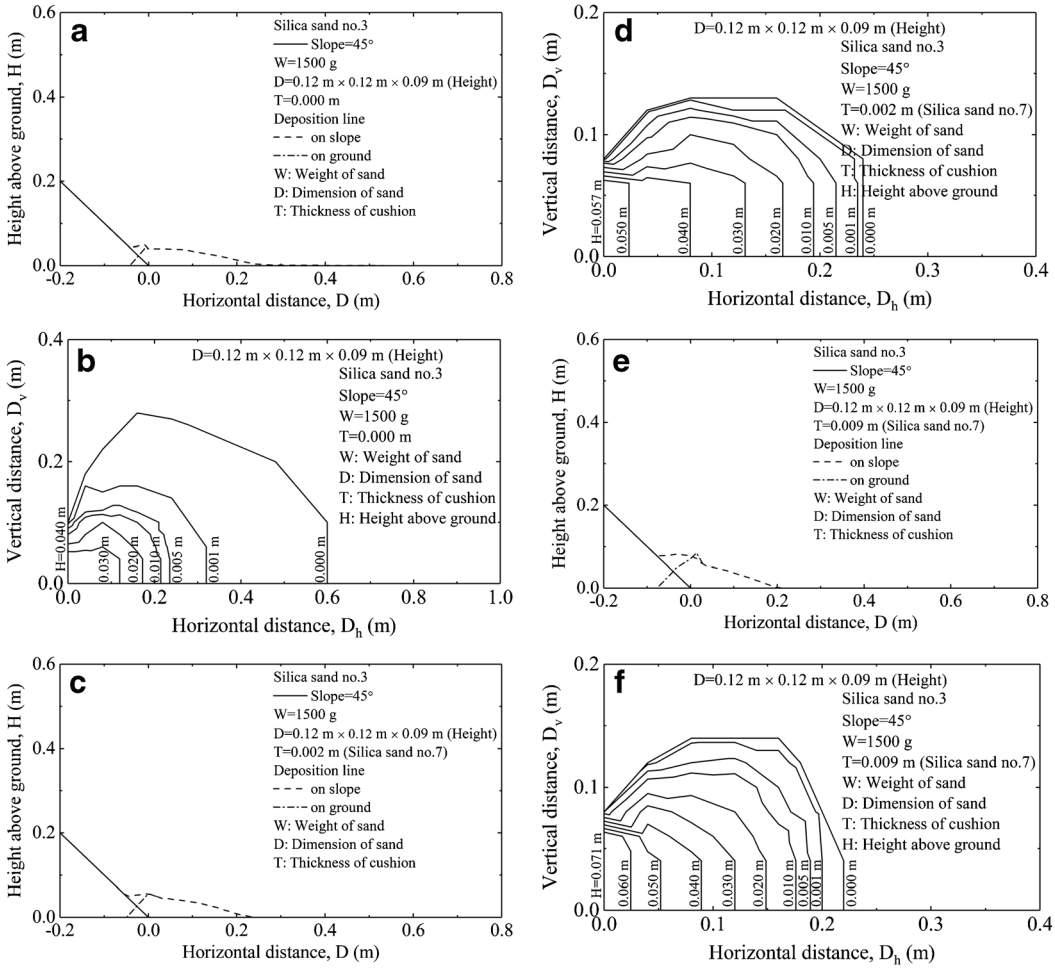

Fig. 13 Effect of cushion on deposition of granular flow of silica sand no. 3 1500 g along a slope of 45°. **a** Deposition in height above ground against horizontal distance with a 0.000-m-thick cushion. **b** Deposition in vertical and horizontal distances with a 0.000-m-thick cushion. **c** Deposition in height above ground against horizontal distance with a 0.002-m-thick cushion. **d** Deposition in vertical and horizontal distances with a 0.002-m-thick cushion. **e** Deposition in height above ground against horizontal distance with a 0.009-m-thick cushion. **f** Deposition in vertical and horizontal distances with a 0.009-m-thick cushion

In Fig. 14(a), an increase in the thickness of cushion led to a gradual increase of the drop height of mass center followed by a decrease of the runout distance of mass center. However, in Fig. 14(b), it showed a decrease of the maximum runout distance of mass at a constant maximum drop height of mass while increasing the thickness of the cushion. An increase in the thickness of cushion resulted in a gradual increase of the angle of mass center movement α_{mc} and the angle of maximum mass movement α_{max} as shown in Fig. 14, with the evidence that the cushion resulted in decrease of runout distance of mass center to thicken the deposition in Fig. 13, which demonstrates that the cushion impaired the mobility of granular flow by consuming the kinetic energy of granular flow. In fact, the substrate materials as a cushion on the path of granular flow would be interacted commonly with granular flow, which may impair its mobility by consuming the kinetic energy of granular flow, or may enhance its mobility by strengthening the kinetic energy of granular flow with the entrainment of the substrate materials (e.g., Legros 2002; Crosta et al. 2009; Farin et al. 2014).

Effect of granular structure on mobility and deposition of granular flow

In reality, granular material would be always in different granular structures, i.e., the grain-void distributions that affect greatly its mobility and deposition. Silica sand no. 3 and silica sand no. 7 were employed to prepare three mixed structures of silica sand no. 3 and silica sand no. 7, i.e., silica sand no. 3 750 g and silica sand no. 7 750 mixed uniformly in simulating the uniform structure, silica sand no. 3 750 in the upper half and silica sand no. 7 750 g in the lower half in simulating the inverse grading structure, silica sand no. 7 750 in the upper half and silica sand no. 3 750 g in the lower half in simulating the normal grading structure, to investigate the effect of granular structure on the mobility and deposition of granular flow along a slope of 45°.

In Fig. 15, for the mixed structures of silica sand no. 3 and silica sand no. 7, the tests in the uniform structure showed a smaller deposition coverage than the tests in the inverse grading structure and normal grading structure, but the maximum thickness of disposition for the tests in the uniform structure is

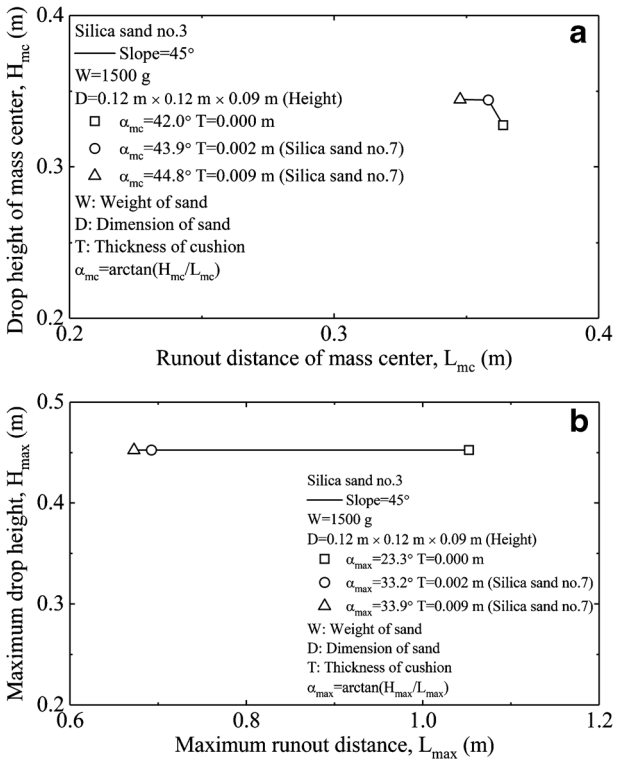

Fig. 14 Drop height of mass against runout distance of mass for silica sand no. 3 1500 g along a slope of 45° with cushion on the ground. **a** Drop height of mass center against runout distance of mass center. **b** Maximum drop height of mass against maximum runout distance of mass

smaller than that for the test in the inverse grading structure but is larger than that for the test in the normal grading structure. For the uniform structure, the visual observation showed a uniform deposition that may include grain segregation in some extent, as illustrated in Fig. 15(a) and (b). However, for the inverse grading structure in Fig. 15(c) and (d) and the normal grading structure in Fig. 15(e) and (f), it showed an inverted structure of the original grading structures in the near runout area but with the deposition of the materials in the upper half of the original grading structures in the far runout area, i.e., the deposition of silica sand no. 7 in the upper layer and silica sand no. 3 in the lower layer in the near runout area and the deposition of silica sand no. 3 in the far runout area for the inverse grading structure as shown in Fig. 15(c) and (d), the deposition of silica sand no. 3 in the upper layer and silica sand no. 7 in the lower layer in the near runout area, and the deposition of silica sand no. 7 in the far runout area for the normal grading structure as shown in Fig. 15(e) and (f).

In Fig. 16(a), the angle of mass movement α_{mc} showed a gradual decrease with the change in turn of the inverse grading structure, the uniform structure, and the normal grading structure, implying a gradual increase of the mobility of granular flow. However, the angle of mass movement α_{max} is kept as a constant of 25° with showing the constant maximum drop height and maximum runout distance of mass despite of their different characteristics of the deposition, as shown in Fig. 16(b). In view of the great effect of granular structure on the mobility of granular flow, the granular structure should be considered for assessment of the mobility of granular flow in reality, especially for the large granular accumulation in high position with specific granular structure.

Effect of granular size on mobility and deposition of granular flow

In reality, during granular flow process down a given slope, granular materials in different granular sizes yield different energies, affecting greatly the mobility and deposition characteristics of granular flow. For a designated amount of sand along a given slope, it showed larger angle of mass movement α_{mc} for silica sand no. 7 than that for silica sand no. 3, as illustrated in Figs. 10(a) and 12(a), implying a stronger mobility of granular flow with larger-sized sands because of the larger kinetic energy in the larger-sized sands.

In addition, Fig. 17 shows the evolution of the drop height of mass against runout distance of mass for silica sand no. 7 1500 g in the uniform structure, silica sand no. 3 750 g and silica sand no. 7 750 g mixed in uniformity, and silica sand no. 3 1500 g in the uniform structure along a slope of 45°, to investigate the effect of granular size on the mobility of granular flow. In Fig. 17(a), the angle of mass movement α_{mc} showed a gradual decrease with the change in turn of silica sand no. 7 in uniformity, silica sand no. 3 and silica sand no. 7 in the mixed uniformity, and silica sand no. 3 in uniformity that resulted in a gradual increase of grain sizes of sand, exhibiting an inverse V-shaped change of the relation of the drop height of mass center and the runout distance of mass center. It is concluded that, for a given uniform structure of sand, the mobility of granular flow increases while increasing the grain sizes of sand. However, the angle of mass movement α_{max} is revealed to decrease gradually while changing in turn silica sand no. 7 in uniformity, silica sand no. 3 and silica sand no. 7 in the mixed uniformity, and silica sand no. 3 in uniformity, showing an increased maximum runout distance at a constant maximum drop height, as shown in Fig. 17(b). Evidently, the granular sizes have showed a great effect on the mobility of granular flow. As a result, the granular sizes of granular materials should be also investigated in detail for assessment of the mobility of granular flow in reality.

Conclusions

A number of flume tests were conducted by promptly removing the gate of the granular container to release the granular materials, i.e., silica sand no. 3 and silica sand no. 7, in simulating granular flow along a designated slope of the flume followed by a level ground, to comprehensively investigate the effects of angle of slope, granular volume, cushion, granular structure, and granular size on the mobility and deposition characteristics of granular flow. In this paper, the major conclusions can be drawn as follows:

1. Along a given slope, the angle of mass movement α_{mc} increased while increasing the amount of sand, implying that an increase of the amount of sand impaired its mobility. However, the angle of mass movement α_{max} decreased while increasing the amount of sand to show an increase of the mobility of sand. By comparison, the angle of mass movement α_{mc} was regarded as being more reliable assessment for the mobility of granular flow in comparison with the angle of mass movement α_{max}.

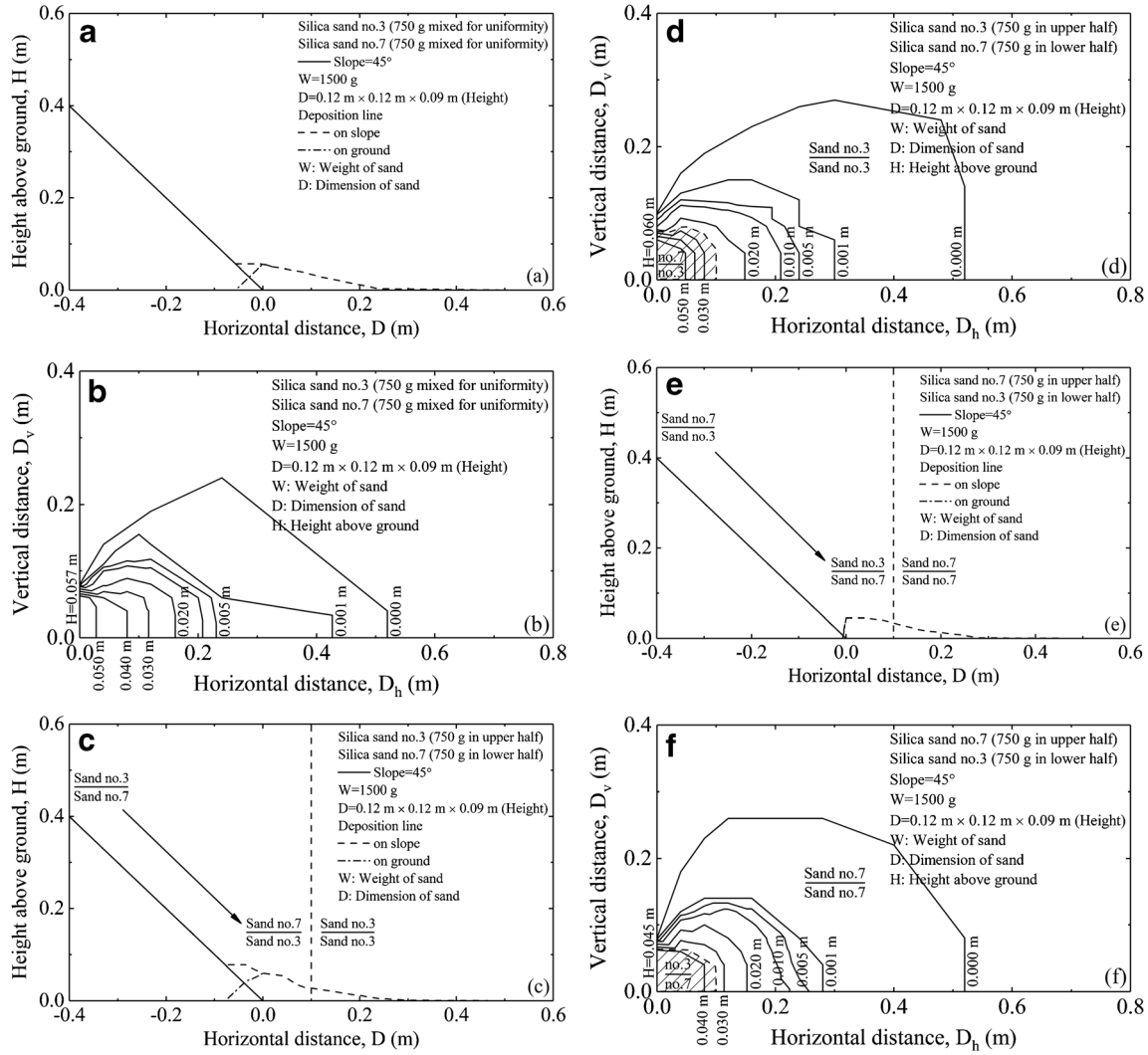

Fig. 15 Effect of granular structure on deposition of granular flow of sand 1500 g along a slope of 45°. **a** Deposition in height above ground against horizontal distance for silica sand no. 3 750 g and silica sand no. 7 750 g mixed in uniformity. **b** Deposition in vertical and horizontal distances for silica sand no. 3 750 g and silica sand no. 7 750 g mixed in uniformity. **c** Deposition in height above ground against horizontal distance for silica sand no. 3 750 g in the upper half and silica sand no. 7 750 g in the lower half. **d** Deposition in vertical and horizontal distances for silica sand no. 3 750 g in the upper half and silica sand no. 7 750 g in the lower half. **e** Deposition in height above ground against horizontal distance for silica sand no. 7 750 g in the upper half and silica sand no. 3 750 g in the lower half. **f** Deposition in vertical and horizontal distances for silica sand no. 7 750 g in the upper half and silica sand no. 3 750 g in the lower half

2. For a given amount of sand along a slope, it showed a V-shaped evolution of the angle of mass movement α_{mc} while increasing the angle of slope, implying the existence of a characteristic combination of the angle of slope and the amount of sand to yield the maximum mobility of granular flow.

3. For a given amount of silica sand no. 3 along a slope of 45° with a cushion on the ground, the angles of mass movement α_{mc} and α_{max} increased while increasing the thickness of cushion, implying that the cushion impaired greatly the mobility of granular flow with the evidence that the cushion resulted in decrease of runout distance of mass center to thicken the deposition.

4. Mobility of granular flow was affected greatly by its granular structure that was prepared by the mixed structures of silica sand no. 3 and silica sand no. 7, i.e., uniform structure, inverse grading structure, and normal grading structure. The maximum thickness of deposition decreased monotonically along the change in turn of the inverse grading structure, the uniform structure, and the normal grading structure. It showed a uniform deposition for the uniform structure of silica sand no. 3 and silica sand no. 7. However, for the inverse grading structure and the normal grading structure of silica sand no. 3 and silica sand no. 7, it showed a deposition in an inverted structure of the original grading structure in the near runout area, but with the deposition of the materials in the upper half of the original grading structure in the far runout area. The angle of mass movement

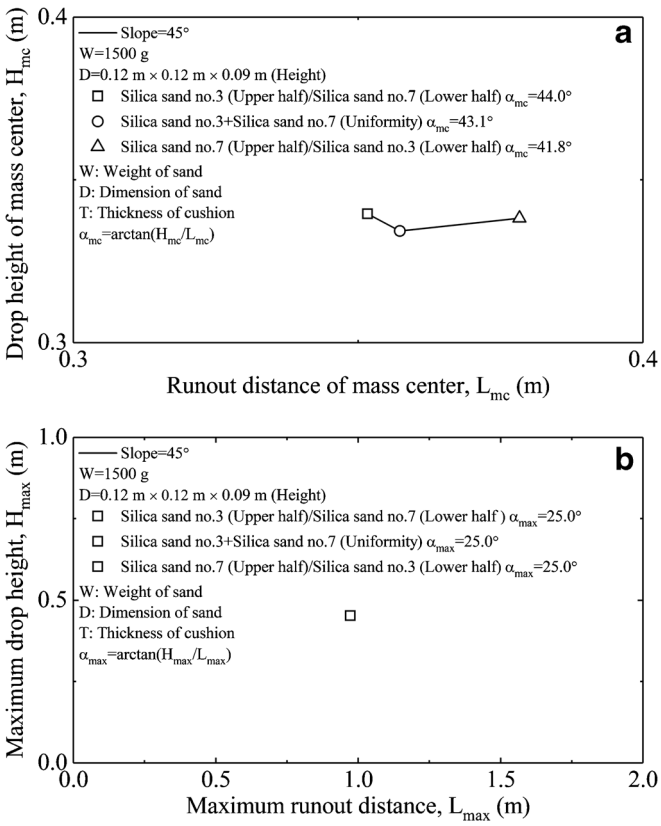

Fig. 16 Drop height of mass against runout distance of mass for the mixed structures of silica sand no. 3 750 g and silica sand no. 7 750 g along a slope of 45°. **a** Drop height of mass center against runout distance of mass center. **b** Maximum drop height of mass against maximum runout distance of mass

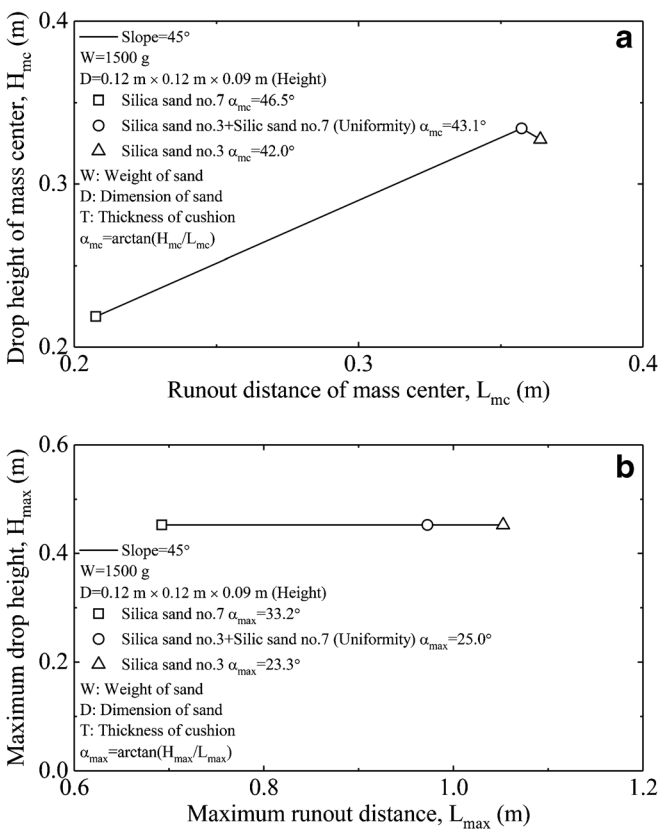

Fig. 17 Drop height of mass against runout distance of mass for the uniform structures of silica sand no. 7 1500 g, silica sand no. 3 750 g and silica sand no. 7 750 g mixed in uniformity, and silica sand no. 3 1500 g along a slope of 45°. **a** Drop height of mass center against runout distance of mass center. **b** Maximum drop height of mass against maximum runout distance of mass

α_{mc} decreased with the change in turn of the inverse grading structure, the uniform structure, and the normal grading structure, implying a gradual increase of the mobility of granular flow.

5. Granular size affected greatly the mobility and deposition of granular flow. For a designated amount of sand along a given slope, the deposition showed larger angle of mass movement α_{mc} for silica sand no. 7 than that for silica sand no. 3, implying the larger-sized materials enhanced the mobility of granular flow. The results of the uniformed structure of silica sand no. 7 and/or silica sand no. 3, for a given amount of sand along a slope of 45°, showed a decrease of the angle of mass movement α_{mc} with the change in turn of silica sand no. 7 in uniformity, silica sand no. 3 and silica sand no. 7 in the mixed uniformity, and silica sand no. 3 in uniformity; i.e., the mobility of granular flow increased while increasing the granular sizes of granular materials.>

Acknowledgments

A special acknowledgement should be expressed to the Geotechnical Engineering Laboratory of the University of Tokyo, Japan that supported the implementation of the tests in this paper.

FundingThis work was supported by the National Natural Science Foundation of China (Grant no. 41807268), the Strategic Priority Research Program of the Chinese Academy of Sciences - China (Grant no. XDA20030301), the "Belt & Road" International Cooperation Team for the "Light of West" Program of CAS - China (Su Lijun), and the Youth Innovation Promotion Association of Chinese Academy of Sciences - China (Grant no. 2018408).

References

ASTM D2487-11 (2011) Standard practice for classification of soils for engineering purposes (Unified Soil Classification System). ASTM International, West Conshohocken

Berger C, McArdell BW, Schlunegger F (2011) Direct measurement of channel erosion by debris flows, Illgraben, Switzerland. J Geophys Res Earth Surf 116(F1):F01002

Boultbee N, Stead D, Schwab J, Geertsema M (2006) The Zymoetz River rock avalanche, June 2002, British Columbia, Canada. Eng Geol 83(1-3):76–93

Buettner KE, Guo Y, Curtis JS (2020) Development of a collisional dissipation rate model for frictional cylinders. Powder Technol 365:83–91

Campbell CS (2006) Granular material flows-an overview. Powder Technol 162(3):208–229

Choi CE, Cui Y, Liu LHD, Ng CWW, Lourenco SDN (2017) Impact mechanisms of granular flow against curved barriers. Geotech Lett 7(4):330–338

Crosta GB, Imposimato S, Roddeman D (2009) Numerical modelling of entrainment/deposition in rock and debris-avalanches. Eng Geol 109(1-2):135–145
Cruden DM, Hungr O (1986) The debris of the Frank slide and theories of rockslide-avalanche mobility. Can J Earth Sci 23(3):425–432
Davies TRH (1982) Spreading of rock avalanche debris by mechanical fluidization. Rock Mech 15:9–24
Davies TRH, McSaveney MJ (1999) Runout of dry granular avalanches. Can Geotech J 36(2):313–320
Eisbacher GH (1979) Cliff collapse and rock avalanches (sturzstroms) in the Mackenzie Mountains, northwestern Canada. Can Geotech J 16(2):309–334
Farin M, Mangeney A, Roche O (2014) Fundamental changes of granular flow dynamics, deposition, and erosion processes at high slope angles: insights from laboratory experiments. J Geophys Res Earth Surf 119(3):504–532
Federico F, Cesali C (2019) Effects of granular collisions on the rapid coarse-grained materials flow. Geotech Lett 9(3):278–283
Gray JMNT (2018) Particle segregation in dense granular flows. Annu Rev Fluid Mech 50:407–433
Hewitt K (1988) Catastrophic landslide deposits in the Karakoram Himalaya. Science 242:64–67
Hsu KJ (1975) Catastrophic debris streams (Sturzstroms) generated by rockfalls. Geol Soc Am Bull 86(1):129–140
Iverson RM, Reid ME, Lahusen RG (1997) Debris-flow mobilization from landslides. Annu Rev Earth Planet Sci 25(1):85–138
JGS 0111 (2015) Test method for density of soil particles. In: Japanese Geotechnical Society Standards: Laboratory Testing Standards of Geomaterials, vol 1. The Japanese Geotechnical Society, Tokyo
JGS 0131 (2015) Test method for particle size distribution of soils. In: Japanese Geotechnical Society Standards: Laboratory Testing Standards of Geomaterials, vol 1. The Japanese Geotechnical Society, Tokyo
JGS 0161 (2015) Test method for minimum and maximum densities of sands. In: Japanese Geotechnical Society Standards: Laboratory Testing Standards of Geomaterials, vol 1. The Japanese Geotechnical Society, Tokyo
Jiang YJ, Fan XY, Li T, Xiao SY (2018) Influence of particle-size segregation on the impact of dry granular flow. Powder Technol 340:39–51
Langroudi MK, Turek S, Ouazzi A, Tardos GI (2010) An investigation of frictional and collisional powder flows using a unified constitutive equation. Powder Technol 197(1-2):97–101
Legros F (2002) The mobility of long-runout landslides. Eng Geol 63:301–331
McCoy SW, Tucker GE, Kean JW, Coe JA (2013) Field measurement of basal forces generated by erosive debris flows. J Geophys Res Earth Surf 118(2):589–602
Ng CWW, Choi CE, Koo RCH, Goodwin GR, Song D, Kwan JSH (2018) Dry granular flow interaction with dual-barrier systems. Géotechnique 68(5):386–399
Ng CWW, Choi CE, Goodwin GR (2019) Froude characterization for unsteady single-surge dry granular flows: impact pressure and runup height. Can Geotech J 56(12):1968–1978
Norem H, Locat L, Schielddrop B (1990) An approach to the physics and the modeling of submarine flowslides. Mar Geotechnol 9(2):93–111
Schürch P, Densmore AL, Rosser NJ, McArdell BW (2011) Dynamic controls on erosion and deposition on debris-flow fans. Geology 39(9):827–830
Strom AL (2004) Rock avalanches of the Ardon River valley at the southern foot of the Rocky Range, Northern Caucasus, North Osetia. Landslides 1:237–241
Thornton C (1997) Coefficient restitution for collinear collisions of elastic perfectly plastic spheres. J Appl Mech 64(2):383–386
Zhou GGD, Ng CWW (2010) Numerical investigation of reverse segregation in debris flows by DEM. Granul Matter 12:507–516
Zhou GGD, Sun QC (2013) Three-dimensional numerical study on flow regimes of dry granular flows by DEM. Powder Technol 239:115–127
Zuo L, Lourenco SDN, Baudet BA (2019) Experimental insight into the particle morphology changes associated with landslide movement. Landslides 16(4):787–798

F. Yu · L. Su
Key Laboratory of Mountain Hazards and Earth Surface Process of CAS, Institute of Mountain Hazards and Environment,
Chinese Academy of Sciences,
Chengdu, 610041, China

F. Yu
e-mail: fwyuui@gmail.com

F. Yu · L. Su
CAS Center for Excellence in Tibetan Plateau Earth Sciences,
Chinese Academy of Sciences,
Beijing, 100101, China

F. Yu · L. Su
China-Pakistan Joint Research Center on Earth Sciences,
CAS-HEC,
Islamabad, 45320, Pakistan

F. Yu · L. Su (✉)
University of Chinese Academy of Sciences,
Beijing, 100049, China
Email: sulijun1976@163.com

F. Yu
Department of Civil Engineering,
The University of Tokyo,
Tokyo, 113-8656, Japan